

國立交通大學

電子工程學系 電子研究所碩士班

碩士論文

MIMO OFDM 系統訊號偵測技術之研究

On Signal Detection of MIMO OFDM Systems



研究生：林觀易

指導教授：陳紹基 博士

中華民國九十四年六月

MIMO OFDM 系統訊號偵測技術之研究

On Signal Detection of MIMO OFDM Systems

研究生：林觀易

Student : Guan-Yi Lin

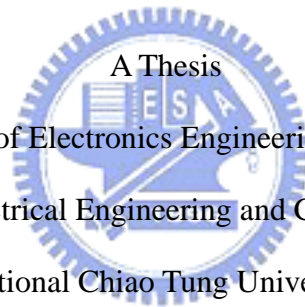
指導教授：陳紹基 博士

Advisor : Sau-Gee Chen

國立交通大學

電子工程學系 電子研究所碩士班

碩士論文



Submitted to Department of Electronics Engineering & Institute of Electronics

College of Electrical Engineering and Computer Science

National Chiao Tung University

in Partial Fulfillment of the Requirements

for the Degree of

Master of Science

in

Electronics Engineering

June 2005

Hsinchu, Taiwan, Republic of China

中華民國九十四年六月

MIMO OFDM 系統訊號偵測技術之研究

學生：林觀易

指導教授：陳紹基 博士

國立交通大學

電子工程學系 電子研究所碩士班

摘 要

本論文討論 MIMO-OFDM 訊號偵測的相關技術，並介紹 V-BLAST 應用在 OFDM 上的文獻。由於連續通道間響應都非常相似，我們提出新的演算法來簡化其他訊號偵測的方法，像是線性偵測與 SQRD 偵測。然後我們做了複雜度比較和位元錯誤率(BER)效能模擬。我們提出的演算法權衡運算複雜度與位元錯誤率，可以達到低成本的架構。接著提出一個方法來預測最少連續幾個 subcarrier 可以使用同一個通道響應。根據這個方法，可以減少系統複雜度但是不會增加錯誤率。

On Signal Detection of MIMO OFDM Systems

Student: Guan-yi Lin

Advisor: Sau-Gee Chen

Department of Electronics Engineering & Institute of Electronics
National Chiao Tung University

Abstract

In this thesis, signal detection techniques of MIMO OFDM system are investigated. Current papers about applications of V-BLAST and OFDM are studied. Based on similarity of response of consecutive sub-channels, new algorithms are proposed to simplify other detection techniques, such as linear detection and SQRD detection. Then complexity comparisons and bit error rate (BER) performance simulations are conducted. The proposed algorithm trade-off complexity and performance for cost-effective architectures. We then propose a scheme to predict minimum number of consecutive subcarriers sharing the same channel response. According to this, system complexity can be largely reduced without loss of BER performance.

誌謝

對於能夠順利完成我的碩士學位，首先要感激的是我的指導教授陳紹基博士，在這兩年中對於我的課業研究著實提供了許多幫助，在我感到困惑時，適時的引導正確的方向，就像迷航的船隻驚見遠方明亮的燈塔那般；另外在生活上也使得我成長不少，在此獻上由衷的感激。

另外要感謝的就是 429 實驗室的夥伴們，伴我度過兩年的研究所生涯，陪同我、一起玩樂、以及一起苦悶。我不能想像如果這兩年沒有你們這群朋友，我的生活將會是怎麼樣？世民、元志、大條、小劉以及承穎，兩年之中，我們大概有四分之三的時間是在一起努力的，謝謝你們；建全學長，卓卓學長兩位學長給我很多建議，非常感謝。雖然要畢業了，但是希望能夠在未來多聚聚。

最後，要感謝這兩年默默支持我的家人，給我許多呵護跟包容，使得我能夠順利的完成學業，謝謝。

Contents

中文摘要.....	I
ABSTRACT.....	II
誌謝.....	III
CONTENTS.....	IV
LIST OF TABLES	VI
LIST OF FIGURES	VII
Chapter 1 Introduction	1
1.1 Background.....	1
1.2 Motivations	3
1.3 Organization of the Thesis	3
Chapter 2 OFDM and MIMO Fundamentals	5
2.1 OFDM System Models	5
2.1.1 Continuous Time Model	6
2.1.2 Discrete Time Model.....	8
2.1.3 Effect of Cyclic Prefix	9
2.2 Concept of Multiple-Input Multiple-Output (MIMO) Systems.....	10
2.2.1 MIMO System Model.....	10
2.3 Signal Detection Algorithms for MIMO Systems	12
2.3.1 Maxima-Likelihood (ML) Detection	13
2.3.2 Suboptimal Algorithms	13
2.3.2.1 The Linear Detection Method.....	13
2.3.2.2 The V-BLAST Detection Method.....	14
2.3.2.3 The SQRD Detection Method.....	16
Chapter 3 MIMO Application to OFDM	19
3.1 MIMO-OFDM Architecture.....	19
3.2 Simplified Data Detection Algorithms for MIMO OFDM Systems.....	21
3.2.1 Boubaker's Algorithm [13]	21
3.2.2 Liu's Algorithm [19]	22
3.3 Introduction to WWiSE 802.11n Proposal.....	23
Chapter 4 The Proposed Data Detection Algorithms	27
4.1 The Simplified Linear Detection Methods.....	27
4.2 The Simplified V-BLAST Detection Method	29

4.3 The Simplified SQRD Detection Methods	31
4.4 Complexity Analysis and Comparison.....	33
4.4.1 Number of Complex Multiplications	34
4.4.2 Number of Complex Additions	35
Chapter 5 Simulation Results	37
5.1 Performance – Execution Time.....	38
5.2 Performance – Bit Error Rate	40
Chapter 6 Conclusion	51
Bibliography	53



List of Tables

Table 3.1 Parameters and specifications of 802.11a system [22]	23
Table 4.1 Multiplication complexities of various detection algorithm for channel inversion	34
Table 4.2 Multiplication complexities of various detection algorithms for data detection	35
Table 4.3 Addition complexities of various detection algorithms for channel inversion	35
Table 4.4 Addition complexities of various detection algorithms for data detection	36
Table 5.1 Simulated WWiSE system parameters	38
Table 5.2 Indoor channel model [23] with short delays, office	41
Table 5.3 Indoor channel model 3 [21], large hall	45



List of Figures

Figure 2.1 Cyclic prefix of an OFDM symbol	6
Figure 2.2 Spectrum of OFDM signal	7
Figure 2.3 (a) Continuous-time OFDM baseband modulator	7
Figure 2.3 (b) Continuous-time OFDM baseband demodulator	7
Figure 2.4 Discrete-time OFDM system model	9
Figure 2.5 Wireless MIMO transmission model	12
Figure 3.1 Transmitter architecture of MIMO OFDM system [12]	20
Figure 3.2 System achitecture of an OFDM and V-BLAST receiver [12]	21
Figure 3.3 Frame structure of 802.11a [22]	24
Figure 3.4 Cyclical delay format of the preamble in WWiSE [21]	25
Figure 4.1 Scenario of the proposed simplified linear detection algorithm 1	28
Figure 4.2 Scenario of the proposed simplified linear detection algorithm 2	28
Figure 4.3 The simplified V-BLAST detection algorithm in [13]	29
Figure 4.4 Scenario of the proposed simplified V-BLAST detection algorithm	30
Figure 4.5 Scenario of the proposed simplified SQRD detection algorithm 1	31
Figure 4.6 Scenario of the proposed simplified SQRD detection algorithm 2	33
Figure 5.1 Computation time of the linear detection method and its new simplified methods	38
Figure 5.2 Computation time of the SQRD detection method and its new simplified methods	39
Figure 5.3 Computation time of the V-BLAST detection method and its new simplified methods	39
Figure 5.4 BER performance versus detection techniques (4x4), office	41
Figure 5.5 BER performance versus detection techniques (4x5), office	42
Figure 5.6 BER performance versus detection techniques (4x6),office	42
Figure 5.7 BER performance versus the linear detection method and the proposed approximation method, office	43
Figure 5.8 BER performance versus the SQRD detection method and the proposed approximation method, office	43
Figure 5.9 BER performance versus the V-BLAST detection method and the proposed approximation method, office	44
Figure 5.10 BER performance versus detection techniques (4x4) , large hall	45
Figure 5.11 BER performance versus detection techniques (4x5) , large hall	46
Figure 5.12 BER performance versus detection techniques (4x6) , large hall	46
Figure 5.13 BER performance versus the linear detection method and the proposed	

approximation method, large hall	47
Figure 5.14 BER performance versus the SQRD detection method and the proposed approximation method, large hall	47
Figure 5.15 BER performance versus the V-BLAST detection method and the proposed approximation method, large hall	48
Figure 5.16 BER performance versus channel MSE, large hall	50






Chapter 1

Introduction

1.1 Background



The rapid growth of telecommunication service subscribers, the popularization of the Internet, and the increase of personal computing devices give a promising future for universal wireless multimedia and data services, which demands robust, high-bit-rate and wide-area wireless networks. Hence, next-generation wireless personal communication systems are expected to provide ubiquitous high performance transmission over hostile mobile environments regardless of mobility or location although there are still technical problems to be solved for this objective [1]. When realizing broadband wireless systems, those severe effects of frequency-selective fading are difficult to solve [2]. Traditionally, more bandwidth is required for higher data-rate transmission. However it is often impractical or sometimes very expensive to increase bandwidth. OFDM techniques get lot of attraction in wireless transmission in recent years for its advantages in mitigating the detrimental effects of frequency-selective fading [3,4,5].

Recent information theory on multiple input multiple output (MIMO) technology revealed that multipath wireless channels facilitate increase of spectral efficiency, provided that those multipath are sufficiently rich [6,7,8]. In such cases, the channel between each transmit and receive antenna pair is flat and uncorrelated. Space Division Multiplexing (SDM) is a technique that can provide a significant improvement in capacity and the bit error rate (BER) performance. Basically, different parallel data streams are transmitted, at the same time and on the same frequency, using an antenna array. When utilizing multiple antennas at the receiver as well, these data streams, mixed-up by the wireless channel, can be recovered by SDM techniques such as Vertical – Bell Laboratories Layered Space-Time (V-BLAST) [9] and Sorted QR Decomposition (SQRD) [10,11].

These algorithms require flat fading channel between each transmit and receive antenna pair. However, most practical channels are frequency-selective fading so that the performance is degraded. An alternative way, OFDM, turns frequency-selective fading into flat fading and is effective when combined with SDM techniques. [12,13]

Recently, plenty of researches are about applying transmitter and receiver diversity [14,15] and space-time codes [16] to multicarrier techniques. The difference between the combined technique and the previous combined SDM and OFDM technique is that the latter can improve the SNR performance as well as the data rate, because it transmits simultaneously different data the different transmit antennas.

1.2 Motivations

In this thesis, we focus on telecommunication systems with rich scattering channels where SDM techniques have best performance. In addition, OFDM systems are studied, because it helps to turn the frequency-selective fading into flat fading conditions. It is known that for each OFDM subcarrier, transmitted signal experience flat fading channel. It is in correspondence to assumed condition when using assumptions V-BLAST and SQRD techniques. If a channel coherence bandwidth is wide, channel gains between subcarriers are similar to each other, where some simplification techniques can be developed, extended and applied to data decoding. Accordingly, we proposed some simplified algorithms for linear detection, V-BLAST detection, and SQRD detection. To get knowledge on computational complexity and BER performance of proposed algorithms, 802.11n systems using both OFDM and MIMO are simulated. Simulation results reveal that the algorithms reduce system complexities with very small BER performance degradation.



1.3 Organization of the Thesis

First, fundamentals of both OFDM and MIMO are studied in chapter 2, and so are the techniques for MIMO data detection. Secondly, the combination of OFDM and MIMO is described in chapter 3, followed by some existed simplification algorithms for data detection. Chapter 4 introduces the new simplified MIMO OFDM data detection algorithms from some major existed algorithms and other detection techniques as well, while chapter 5 includes simulations. Finally, we conclude with some remarks of the work in chapter 6.



Chapter 2

OFDM and MIMO Fundamentals

2.1 OFDM System Models

The principle of multicarrier system is to separate the data stream into several parallel ones, each modulated by a specific subcarrier and discrete Fourier Transform (DFT) is used in the baseband modulation and demodulation. Through this approach, only a pair of oscillator (for I-part and Q-part) is needed instead of multiple oscillators to modulate different signals at different carriers.

When signals pass through a time-dispersive channel, inter-symbol interference (ISI) and inter-carrier interference (ICI) usually occur in the receiver and cyclic prefix (CP) was introduced to combat ISI and ICI. Cyclic prefix, shown in Figure 2.1, is a copy of the tail part of a symbol, which is inserted in between the symbol to be transmitted and its preceding symbol. As long as the cyclic prefix length is longer than its experiencing time-dispersive channel length, ISI can be avoided. At the same time, the cyclic prefix along with its symbol makes a periodic signal and maintains the properties of circular convolution and subcarrier orthogonality that prevents the ICI effect.

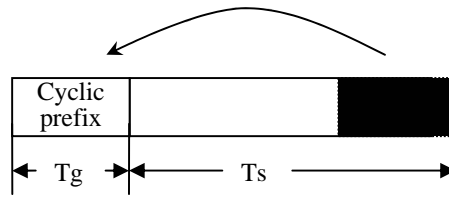


Figure 2.1 Cyclic prefix of an OFDM symbol

2.1.1 Continuous Time Model

In this section, a continuous-time model is used to introduce the whole OFDM baseband system including the transmitter and receiver. In the transmitter, the transmitted data is split into multiple subchannels with overlapping frequency bands.

The spectrum of OFDM signal is shown in Figure 2.2. It is clear that the spectrum of each subchannel is spreading to all the others, but is zero at all other subcarrier frequencies, because of the sinc function property, which is the key feature of the orthogonality.

Figure 2.3 (a) shows a typical continuous-time OFDM baseband modulator, in which the transmitted data is split into multiple parallel streams which are modulated by different subcarriers and then transmitted simultaneously.. At the receiver, the received signal is demodulated simultaneously by multiple matched filters and then the data on each subchannel is obtained by sampling the outputs of matched filters, as shown in Figure 2.3 (b).

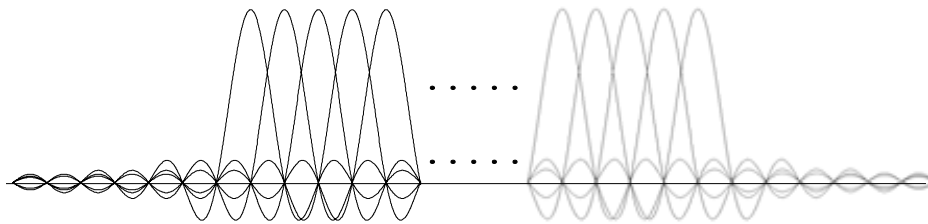


Figure 2.2 Spectrum of an OFDM signal

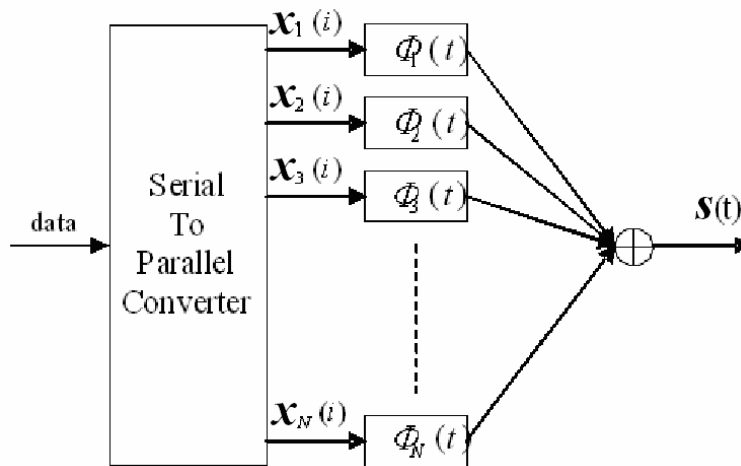


Figure 2.3 (a) Continuous-time OFDM baseband modulator

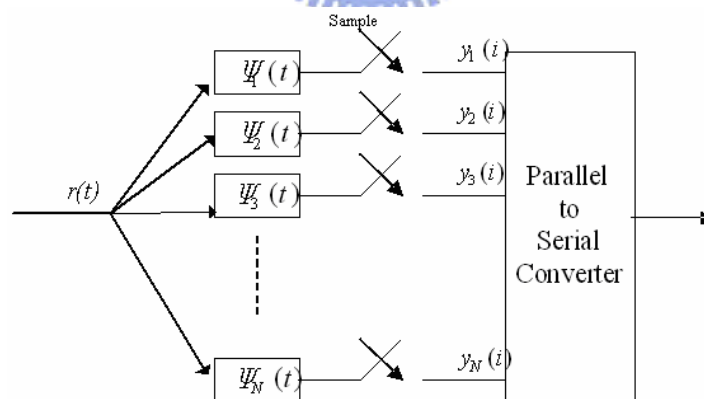


Figure 2.3 (b) Continuous-time OFDM baseband demodulator

2.1.2 Discrete Time Model

As mentioned previously, to simultaneously transmit multiple data, the transmitter must modulate data with multiple subcarriers and the receiver must demodulate with multiple matched filters. In fact, the modulation and demodulation can be implemented efficiently by using digital IDFT/DFT operations, because they can be respectively represented as

$$\begin{aligned} s(i) &= \sum_{k=0}^{N-1} x(k) e^{j \frac{2\pi}{N} ki} \\ &= \sum_{k=0}^{N-1} x(k) \phi_k(i) \end{aligned} \quad (2.1)$$

$$\begin{aligned} y(i) &= \sum_{k=0}^{N-1} r(k) e^{-j \frac{2\pi}{N} ki} \\ &= \sum_{k=0}^{N-1} r(k) \psi_k(i) \end{aligned} \quad (2.2)$$

which are the same as IDFT operation of the transmitted data $x(k)$ and DFT operation of the received data $r(k)$, respectively.

Figure 2.4 shows the discrete-time baseband OFDM model. The IDFT transforms the frequency-domain data into time-domain data which is delivered over the air and experiences multi-path channel, denoted as $h(n, m)$. At the receiver, to recover the signal in frequency domain, DFT is adopted in the demodulator as a matched filter. Then the frequency domain signal of each subchannel is obtained from its DFT output.

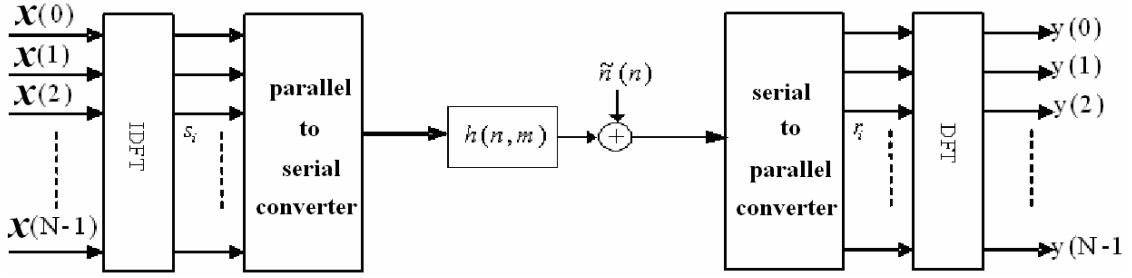


Figure 2.4 Discrete-time OFDM system model

2.1.3 Effect of Cyclic Prefix

Assume the given channel is quasi-static, i.e., constant during the transmission of an OFDM symbol and variable symbol wise, where the quasi-static impulse response is $h(t, \tau)$, t is the time index and τ is the channel path delay. The received signal $r(t)$ can be expressed as

$$r(t) = s(t) * h(t, \tau) + \tilde{n}(t) \quad (2.3)$$

where $s(t)$ is the transmitted data and $\tilde{n}(t)$ is the white Gaussian noise. Because of multipath channels, orthogonality as shown in Figure 2.2 will be destroyed by ISI and ICI. However, as long as the cyclic prefix length is longer than that of $h(n, m)$, ISI effect can be avoided. At the same time, linear convolution of $s(n)$ and $h(n, m)$ turns out to be circular convolution. It is known that circular convolution in time domain results in multiplication in frequency domain when the channel is stationary so that the received signal $y(k)$ in frequency domain is the product of transmitted data $x(k)$ and subcarrier channel response $H(k)$. Thus, the orthogonality is maintained (if $h(n, m)$ is fixed within the symbol length) and data can be easily recovered by one-tap channel equalizer, i.e., dividing $y(k)$ by the corresponding $H(k)$.

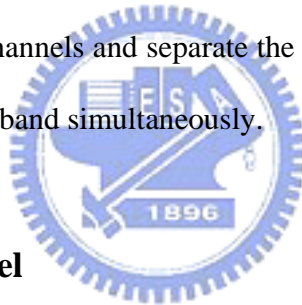
$$y(k) = H(k) \times x(k) + n(k) \quad (2.4)$$

2.2 Concept of Multiple-Input Multiple-Output (MIMO)

Systems

MIMO system architectures provide better spectral efficiency than conventional systems because of the benefit of multiple antenna or space diversity both at the transmitter and receiver.

MIMO systems provide the ability to turn multipath propagation, which is traditionally a drawback of wireless transmission, into a benefit. Since MIMO systems effectively take advantage of random fading and multipath delay spread, the signals transmitted from each transmit antenna appear highly uncorrelated at each receive antenna and the signals travel through different spatial channels. Then the receiver can exploit these different spatial channels and separate the signals transmitted from different antennas at the same frequency band simultaneously.



2.2.1 MIMO System Model

MIMO is a promising technology suited for high-speed broadband wireless communications. Through space division multiplexing, the MIMO technology can transmit multiple data streams in independent parallel spatial channels, thereby increasing the total transmission rate of the system.

MIMO systems can be simply defined. Considering an arbitrary wireless communication system, a link is considered for which the transmitter is equipped with N_t transmit antennas and the receiver is equipped with N_r receive antennas. Such a setup is illustrated in Figure. 2.5. Consider this system, some important assumptions are made first:

1. The channel is constant during the transmission of a packet. It means the communication is carried out in packets that are of shorter time-span than the coherence time of the channel.

2. The channel is memoryless. It means that an independent realization of channel is drawn for each use of the channel.

3. The channel is frequency-flat fading. It means that constant fading over the bandwidth is desired in the case of narrowband transmissions. It also indicates that the channel gain can be represented by a complex number.

4. Only a single user transmits signals at any given time, so the received signal is corrupted by AWGN only.

With these assumptions, it is common to represent the input/output relations of a narrowband, single-user MIMO link by the complex baseband vector notation

$$y = Hx + n \quad (2.5)$$

where x is the $N_t \times 1$ transmit vector, y is the $N_r \times 1$ receive vector, H is the $N_r \times N_t$ channel matrix, and n is the $N_r \times 1$ additive white Gaussian noise (AWGN) vector at some instant in time. All of the coefficients h_{ij} comprise the channel matrix H and represent the complex gain of the channel between the j th transmit antenna and the i th receive antenna.

The channel matrix can be written as

$$H = \begin{pmatrix} h_{11} & h_{12} & \cdots & h_{1N_t} \\ h_{21} & h_{22} & \cdots & h_{2N_t} \\ \vdots & \vdots & \ddots & \vdots \\ h_{N_r 1} & h_{N_r 2} & \cdots & h_{N_r N_t} \end{pmatrix} \quad (2.6)$$

$$h_{ij} = \alpha_{ij} + \beta_{ij}j = |h_{ij}| \cdot e^{j\phi_{ij}} \quad (2.7)$$

Coefficients $\{h_{ij}\}$ reflect unknown channel properties of the medium, usually Rayleigh distributed in a rich scattering environment without line-of-sight (LOS) path. If α and β are independent and Gaussian distributed random variables, then $|h_{ij}|$ is a Rayleigh distributed random variable. Actually, coefficients $\{h_{ij}\}$ are likely to be subject to varying degrees of fading and change over time. Therefore, the determination of the channel matrix is an important and necessary aspect of MIMO processing. If all these coefficients are known, there will be sufficient information for the receiver to eliminate interference from other transmitters operating at the same frequency band.

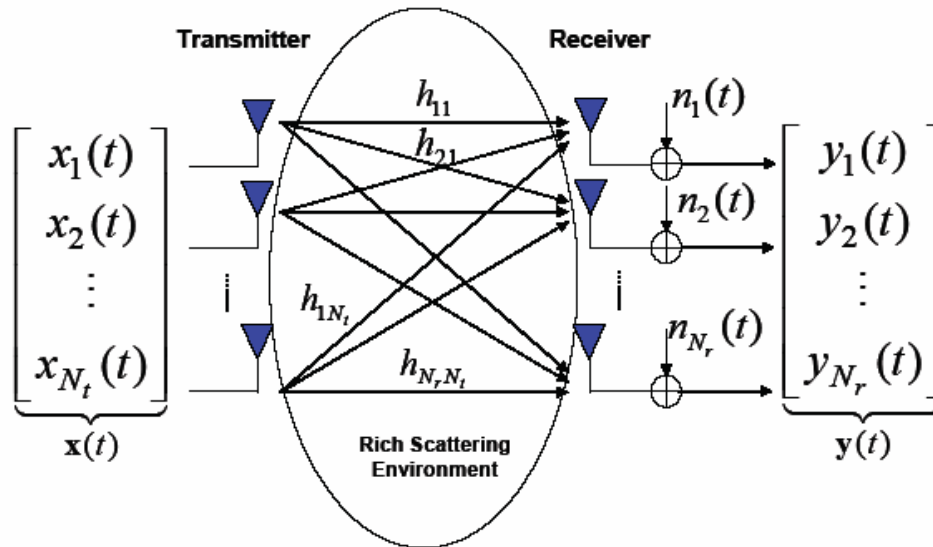


Figure 2.5 Wireless MIMO transmission model [17]

2.3 Signal Detection Algorithms for MIMO Systems

Signal detection here means a process that try to recover the transmitted signals at receivers. As shown in equation 2.5, the task is to detect the transmitted vector x based on received vector y and channel state information (CSI) H .

In this section zero-forcing (ZF) criterion is considered due to consideration of lower complexity. Zero-forcing techniques receive an input vector y and send it to a filter bank which eliminates the mutual interference without caring about noise.

2.3.1 Maxima-Likelihood (ML) Detection

Since modern transmission systems are digital, each element of transmitted vector x is chosen from a finite set, which is denoted as A , such as BPSK, QPSK and 16-QAM. Hence, a transmitted signal x belongs to A^{N_t} . The optimum maximum-likelihood (ML) detector searches over the whole set of transmit signals $x \in A^{N_t}$, and decides in favor of the transmit signal x_{ML} that minimizes the Euclidian distance to the receive vector y , i.e.

$$x_{ML} = \arg \min_{x \in A^{N_t}} \|y - Hx\|^2 \quad (2.8)$$

The computational effort is of order M^{N_t} , where M denotes size of finite set A . When using high modulation scheme or many transmitting antennas, ML detection is impractical.

2.3.2 Suboptimal Algorithms

Although ML detection reaches optimal performance, it is not feasible for large numbers of transmit antennas or high modulation schemes. In the sequel, some suboptimal algorithms are investigated. The target is to find algorithms that have performance near ML and low complexities.

2.3.2.1 The Linear Detection Method

For linear detection method, the received vector y is linearly multiplied with a matrix G , and then a parallel decision follows. Zero-forcing criterion means that mutual

interferences between the transmitted signals shall be perfectly suppressed without concerning noise. As a result, matrix G is generated by the Moore-Penrose pseudo-inverse (denoted by $(\cdot)^+$) of the channel matrix H [18].

$$G_{ZF} = H^+ = (H^H H)^{-1} H^H \quad (2.9)$$

where H is assumed to have full column rank. The parallel decision maps each element of the filtered output vector

$$\tilde{x}_{ZF} = G_{ZF} y = H^+ y = x + (H^H H)^{-1} H^H n \quad (2.10)$$

onto an element of the symbol alphabet through a minimum distance quantization. The estimation errors correspond to the main diagonal elements of the error covariance matrix

$$\phi_{ZF} = E[(\tilde{x}_{ZF} - x)(\tilde{x}_{ZF} - x)^H] = \sigma_n^2 (H^H H)^{-1} \quad (2.11)$$

that equals the covariance matrix of the filtered noise. Small eigenvalues of $H^H H$ will result in large estimation errors owing to noise amplification, which is especially severe in systems with equal number of transmit and receive antennas. Using random matrix theory [19], it can be shown that asymptotically for $N_T = N_R \rightarrow \infty$ the noise amplification tends to infinity.

2.3.2.2 The V-BLAST Detection Method

Vertical – Bell Laboratories Layered Space-Time (V-BLAST) [9] is proposed to improve performance of the linear detection method by utilizing successive interference cancellation based on zero-forcing criterion. It suggests that transmitted signals are detected sequentially rather than in parallel. In each detection step, the signal which yields the smallest estimation error is linearly detected. It is shown in [9] that row g_{ZF} , the row with minimum norm in G_{ZF} , has the largest signal-to-noise ratio (SNR) and yields the smallest estimation error because it causes minimum noise enhancement.

$$\tilde{x}_i = g_{ZF}^i y = g_{ZF}^i (Hx + n) = x_i + \eta_i \quad (2.12)$$

where i means the order index a signal is detected.

The \tilde{x}_i is quantized to x_i , and the interference of this signal is removed by subtracting it from the received signal y and nulling the i -th column of the channel matrix. Nulling and canceling are repeated until all signal is detected, as summarized in the following algorithm steps:

Begin

$$H^1 = H \quad (2.13.a)$$

$$y_1 = y \quad (2.13.b)$$

$$\text{for}(i=1 ; i \leq N_t ; i++) \quad (2.13.c)$$

$$G_{ZF}^i = (H^i)^+ \quad (2.13.d)$$

$$k_i = \arg_i \min \|G_{ZF}^i\| \quad (2.13.e)$$

$$g_{ZF}^i = (G_{ZF}^i)_{k_i} \quad (2.13.f)$$

$$\tilde{x}_{k_i} = g_{ZF}^i y \quad (2.13.g)$$

$$x_{k_i} = \text{quantize}(\tilde{x}_{k_i}) \quad (2.13.h)$$

$$y_{i+1} = y_i - x_{k_i} H_{k_i} \quad (2.13.i)$$

$$H^{i+1} = H_{k_i}^i \quad (2.13.j)$$

$$\text{end} \quad (2.13.k)$$

where $(G)_i$ means i -th row of G , H_{k_i} means k_i -th column of H , and $H_{k_i}^i$ means nulling the k_i -th column of H .

The main computational bottleneck is the computation of pseudo inverse for N_t times. For saving computation, channel response is assumed to be invariant within a packet, as assumption 1 suggests. The optimal detection order and each nulling vector g_{ZF}



is validly used to detect received signals in the whole packet since they share the same channel matrix. That is, pseudo inverse of the channel is not updated

2.3.2.3 The SQRD Detection Method

Although V-BLAST algorithm achieves good performance, it still costs high computation power. The sorted QR decomposition (SQRD) detection algorithm [10,11] is introduced in the sequel based on QR decomposition. SQRD algorithm costs rather lower computation power with small performance degradation. The method's operation is listed below.

The SQRD algorithm [10,11] is an extension to the modified Gram-Schmidt procedure by reordering the columns of the channel matrix before each orthogonalization step. The basic idea is to minimize $|r_{k,k}|$ in the order it is computed (from 1 to N_t) instead of to maximize in the order of detection (from N_t to 1). $|r_{k,k}|$ denotes absolute value of the element at k-th row and k-th column in R matrix. This is motivated because the signal detected last has effects on only few other layers through error propagation and therefore has small SNR's. Since $r_{1,1}$ is simply the norm of the column vector h_1 , the first step in the SQRD algorithm is simply to permute the column of H with minimum norm to this position. During the following orthogonalization of the vectors h_2, \dots, h_{N_t} with respect to the normalized vector h_1 , the first row of R is obtained. In the second step, $r_{2,2}$ is determined in a similar fashion from the remaining N_t-1 orthogonalized vectors, et cetera.

A special note is that the column norms is calculated only once in the beginning and can be easily updated afterwards. Therefore, the computational complexity owing to sorting is negligible. It must be emphasized that SQRD does not always lead to the perfect detection sequence. That is, SQRD has performance degradation compared to V-

BLAST, but in many cases of interest the performance degradation is small compared to the reduced complexity [10,11]

Begin

$$R = 0, Q = H, p = (1, \dots, Nt) \quad (2.14.a)$$

$$\text{for}(i=1 ; i \leq Nt ; i++) \quad (2.14.b)$$

$$\text{norm}_i = \|q_i\|^2 \quad (2.14.c)$$

$$\text{end} \quad (2.14.d)$$

$$\text{for}(i=1 ; i \leq Nt ; i++) \quad (2.14.e)$$

$$k_i = \underset{l = i \dots Nt}{\text{arg min}} \text{norm}_l \quad (2.14.f)$$

$$\text{exchange columns of } i \text{ and } k_i \text{ in } R, p, \text{norm} \quad (2.14.g)$$

$$\text{exchange columns in the first } N_r + i - 1 \text{ rows of } Q \quad (2.14.h)$$

$$r_{i,i} = \sqrt{\text{norm}_i} \quad (2.14.i)$$

$$q_i = \frac{q_i}{r_{i,i}} \quad (2.14.j)$$

$$\text{for}(k=i+1 ; k \leq Nt ; k++) \quad (2.14.k)$$

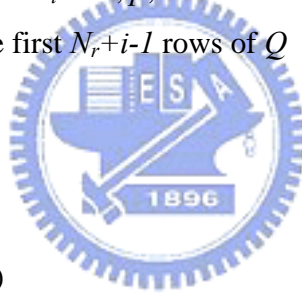
$$r_{i,k} = q_i^H \times q_k \quad (2.14.l)$$

$$q_k = q_k - r_{i,k} \times q_i \quad (2.14.m)$$

$$\text{norm}_k = \text{norm}_k - r_{i,k}^2 \quad (2.14.n)$$

$$\text{end} \quad (2.14.o)$$

$$\text{end} \quad (2.14.p)$$





Chapter 3

MIMO Application to OFDM

Algorithms introduced for MIMO transmission require frequency-flat fading channels, and it limits its application to narrowband transmissions. For real broadband transmission systems, channel conditions are often frequency-selective fading. A technique alleviating severe effect of frequency-selective fading is demanded. OFDM technique is a good solution for this purpose in wireless transmission owing to its advantages [3,4,5].

3.1 MIMO-OFDM Architecture

According to Section 2.1, OFDM turns frequency-selective fading channel into several frequency-flat fading subchannels, solving the major problem in wideband transmission systems. Boubaker et. al [12] proposed MIMO-OFDM using V-BLAST algorithm to detect transmitted signals on each subcarrier. MIMO-OFDM transceiver architectures are also proposed, as shown in Figure 3.1 and 3.2.

Subchannels are orthogonal to each other in OFDM systems. Hence, in single-input-single-output (SISO) OFDM systems, the received signals are product of channel response and transmitted signal, as shown in equation 2.4. In MIMO systems, signals transmitted from different antenna on a subcarrier simultaneously interfere each other, but signals at different subcarriers are independent. At the receiver antennas, a linear combination of the transmitted signal and channel response on each subcarrier is observed, as equation 2.5 shows. That corresponds to assumptions of MIMO systems. On each subchannel, a space division multiplexing (SDM) like V-BLAST is applied. That is, the task is to recover x from the received signal y and channel state information (CSI) H on each subcarrier.

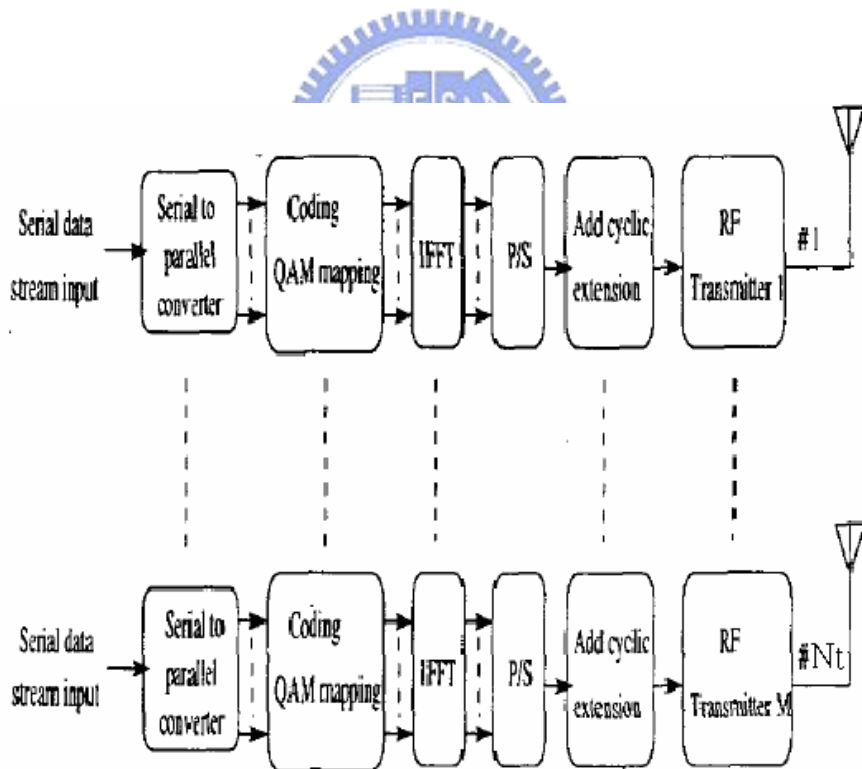


Figure 3.1 Transmitter architecture of MIMO OFDM system [12]

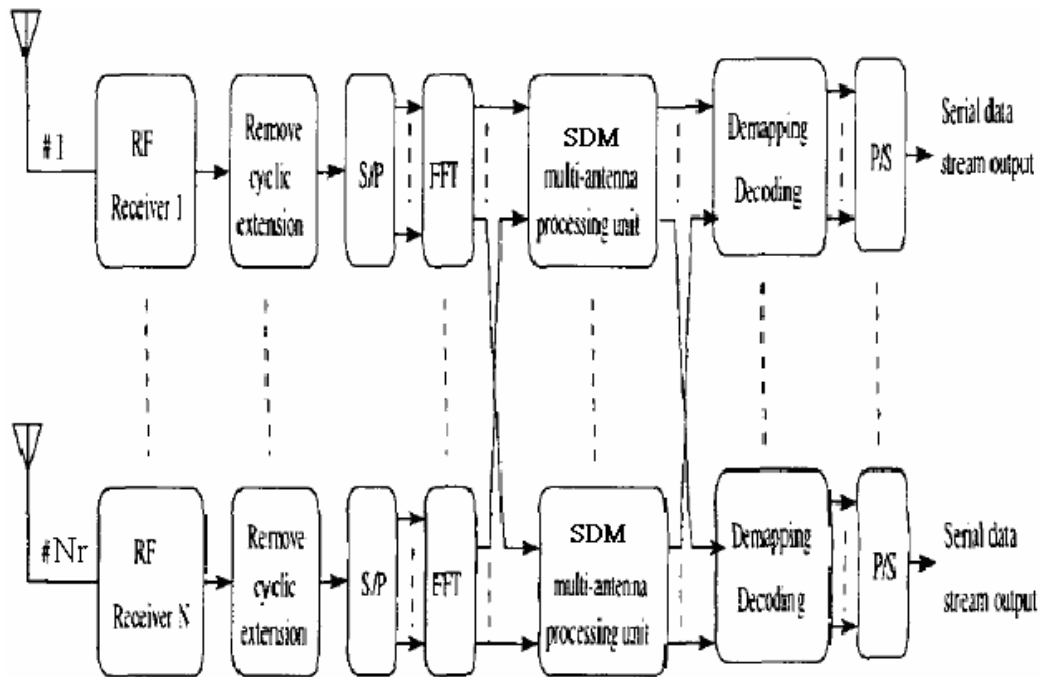


Figure 3.2 System architecture of an OFDM and V-BLAST receiver [12]

3.2 Simplified Data Detection Algorithms for MIMO OFDM Systems

On each subchannel, a V-BLAST or SQRD detector is used since we can formulate the problem as equation 2.5. For most practical OFDM systems, there are too many subcarriers to implement a detector for each subcarrier. Fortunately, channel responses of successive subcarriers are often similar. Some simplified algorithms are proposed based on this observation.

3.2.1 Boubaker's Algorithm [13]

In [13], Boubaker et. al proposed an algorithm based on V-BLAST which divide used subcarriers into groups. Since data detection and channel inversion can be separated to two parts, the same nulling vectors corresponding to a subcarrier of a group is used to

detect data of all the group. That is, the algorithm assumes that the channel conditions on all subcarriers in this group are identical. Therefore, a dramatic reduction of computation cost is obtained. In addition, a new detection algorithm is proposed. A sub-optimal ordering is obtained simply from the first pseudo-inverse by sorting $\|(G^l)_j\|^2$ in an ascending order, for $j = 1, \dots, M$, where $G^l = H^H$. Then, the series of calculations of pseudo-inverse can be replaced by applying Gram-Schmitt Orthogonalization (GSO) once to H , provided that the decoding ordering is known in advance.

3.2.2 Liu's Algorithm [20]

For good channel conditions, [13] provide a good way for both good performance and low complexity, while for slightly poor channels, this may not be enough. Liu and Yang [20] proposed an algorithm for this situation. They use V-BLAST to determine pseudo inverse matrixes at some subcarrier of a group and then use equation 3.1 to approximate pseudo inverse matrixes at other subcarriers.

$$(A - \varepsilon)^+ \approx A^+ + A^+ \varepsilon A^+ \quad (3.1)$$

With equation 3.1, pseudo inverse at $(k+1)$ -th subchannel is calculated by using pseudo inverse of the k -th subchannel.

$$H(k+1)^+ \approx H(k)^+ + H(k)^+ (H(k) - H(k+1))H(k)^+ \quad (3.2)$$

where $H(k)$ is channel response of k -th subchannel.

Other pseudo inverse is also calculated.

$$H(k+1, p)^+ \approx H(k, p)^+ + H(k, p)^+ (H(k, p) - H(k+1, p))H(k, p)^+ \quad (3.2)$$


where $H(k, p)$ is the p -th pseudo inverse of the k -th subchannel. A special note is that $H(k, p)$ has $(p-1)$ columns of zeros, because $(p-1)$ transmitted data are already decoded.

3.3 Introduction to WWiSE 802.11n Proposal

To examine validity of proposed algorithms in next chapter, WWiSE proposal, a proposal for next generation 802.11n standard, is adopted for simulation. 802.11n standard utilize both MIMO and OFDM techniques for efficient wireless LAN. In the following, brief introduction is described.

WWiSE proposal [21] emphasize backward compatibility with existing installed base, building on experience with interoperability in 802.11g and previous 802.11 amendments which are mainly designed for indoor wireless internet applications. Hence, we review the physical layer of wireless LAN 802.11a [22] system which is based on OFDM technology. The main system parameters of IEEE 802.11a Wireless LAN standard are listed in Table 3.1.

Table 3.1 Parameters and specifications of 802.11a system [22]



Signal bandwidth	20MHz
Sample duration	50ns
FFT length	64
Used subcarriers	52
Data subcarriers	48
Pilot subcarriers	4
Symbol period	3.2us (64 samples)
Cyclic prefix	0.8us (16 samples)
Subcarrier spacing	312.5 kHz
Modulation	BPSK, QPSK, 16QAM, 64QAM
Channel coding	1/2 convolutional, constrain length 7, Optional puncturing
Data rate	6, 9, 12, 18, 24, 36, 48, 54 Mbps

In 802.11a standard, a frame is composed of three fields. Figure 3.3 shows the packet format which facilitates synchronization and channel estimation of the receiver. In the preamble field, the preambles are composed of ten repeated short symbols and two repeated long symbols. The total duration of short symbols is 8 μ s and so is that of long symbols. Since the SIGNAL field contains the most important information of the packet, such as frame length and modulation, synchronization and channel estimation must be finished before decoding of the SIGNAL.

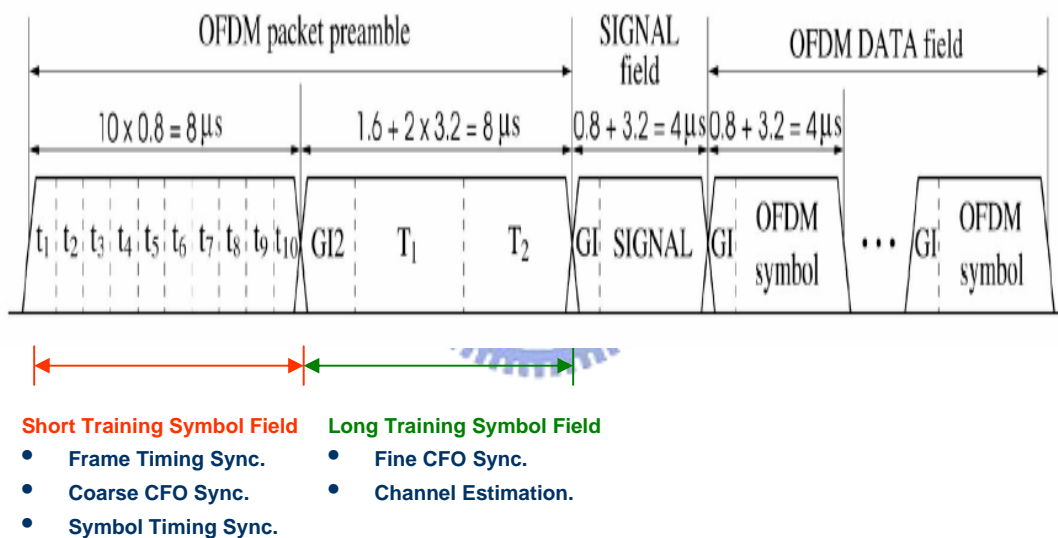


Figure 3.3 Frame structure of 802.11a [22]

For the purpose of compatibility with the 802.11 legacy devices, the legacy part of the preamble format in WWiSE proposal is the same as that in 802.11a. If the legacy preambles are transmitted from multiple antennas, the mapping of this single spatial stream to multiple antennas has to be done such that beamforming in far-field is mitigated. One method for achieving this is to use a cyclical delay diversity (CDD) mapping. The

cyclical delay is adopted in WWiSE proposal, whose format is used for simulation. Figure 3.4 shows the cyclical delay format in WWiSE. The maximum number of the spatial data streams is four.

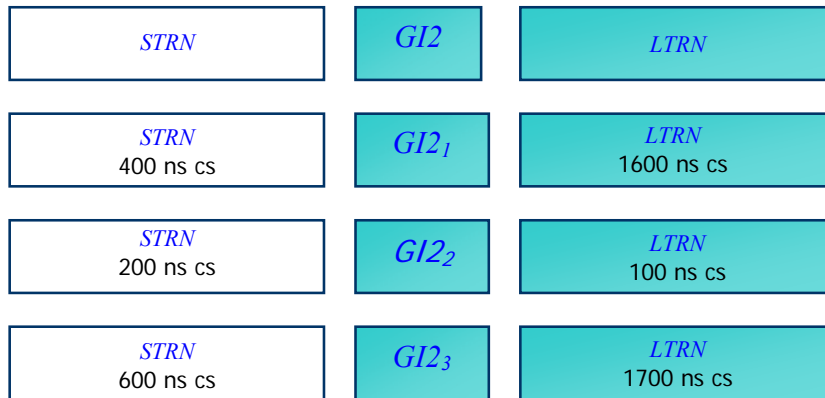


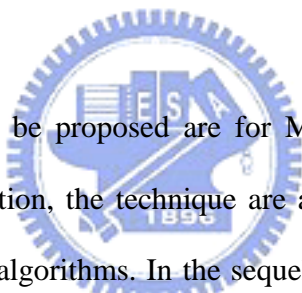
Figure 3.4 Cyclical delay format of the preamble in WWiSE [21]

STRN stands for the short training sequence. LTRN represents the long training symbol. GI2 is the guard interval of the long training symbol.



Chapter 4

The Proposed Data Detection Algorithms



Since the algorithms to be proposed are for MIMO-OFDM systems to reduce complexity of V-BLAST detection, the technique are also useful to simplify the linear detection and SQRD detection algorithms. In the sequel, some simplification algorithms are introduced based on the designs of [13,20]

4.1 The Simplified Linear Detection Methods

In the linear detection method, a received vector is simply multiplied with pseudo inverse of channel. Direct computation of pseudo inverse is costly. Although pseudo inverse is calculated only once for each subcarrier, an approximation with good performance and low cost is highly required, because it is calculated N times for a symbol. Based on the concept of [13], we propose two simplified algorithms. The simplified algorithm 1, for each two subcarriers, compute inverse of one subcarrier, and directly

applies it to the data detection of the other subcarrier. Based on the approximation to pseudo inverse in [20], obviously it is also useful in linear detection. Our proposed linear detection algorithm 2 is that for each two subcarriers, we compute the inverse of one subcarrier, while approximate the other using the computed one.

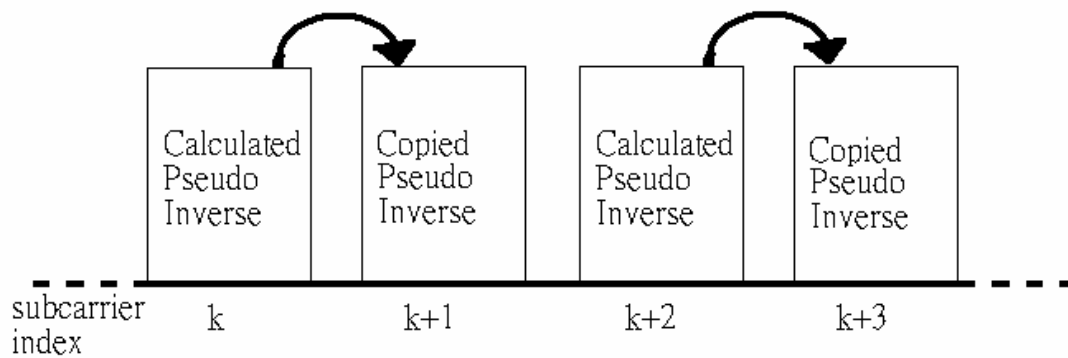


Figure 4.1 Scenario of the proposed linear detection algorithm 1

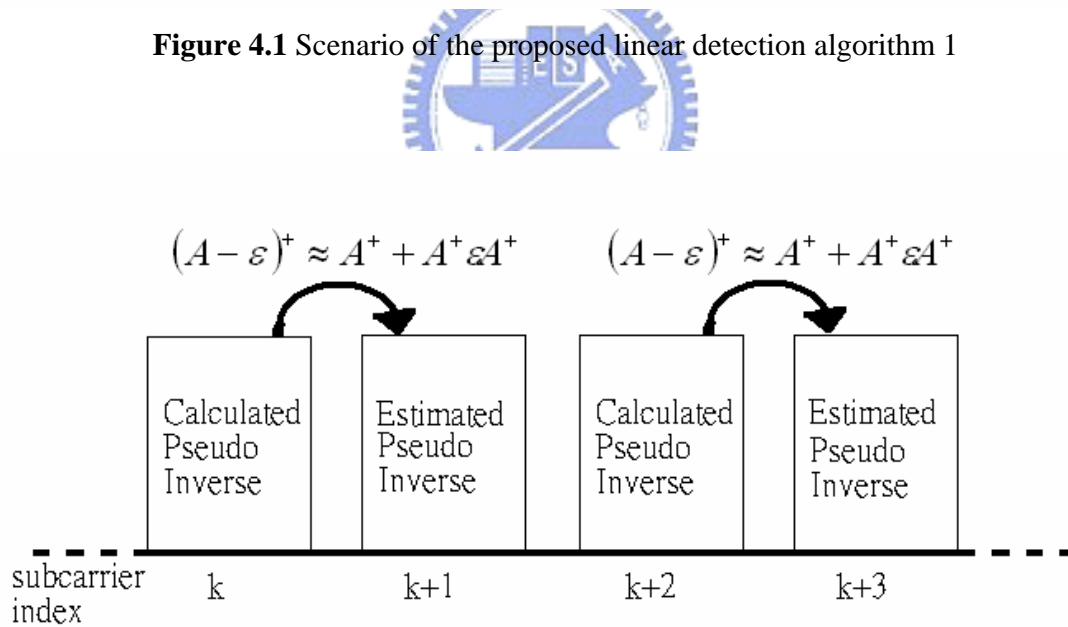


Figure 4.2 Scenario of the proposed linear detection algorithm 2

```

Begin
for(i=1 ; i <= subcarrier number ; i+=2)                                (4.1.a)
     $G_{ZF}^i = (H^i)^+$                                                     (4.1.b)
    if algorithm 1                                                            (4.1.c)
         $G_{ZF}^{i+1} = G_{ZF}^i$                                             (4.1.d)
    else //algorithm 2                                                        (4.1.e)
         $G_{ZF}^{i+1} = G_{ZF}^i + G_{ZF}^i (H^i - H^{i+1}) G_{ZF}^i$           (4.1.f)
    end                                                                        (4.1.g)
end                                                                            (4.1.k)

```

4.2 The Simplified V-BLAST Detection Method

Simplified algorithms for V-BLAST detection method are already proposed in [13,20]. [13] assumed successive subcarriers share a channel response so that vectors of a subcarrier is applied to detect signal of other subcarriers.

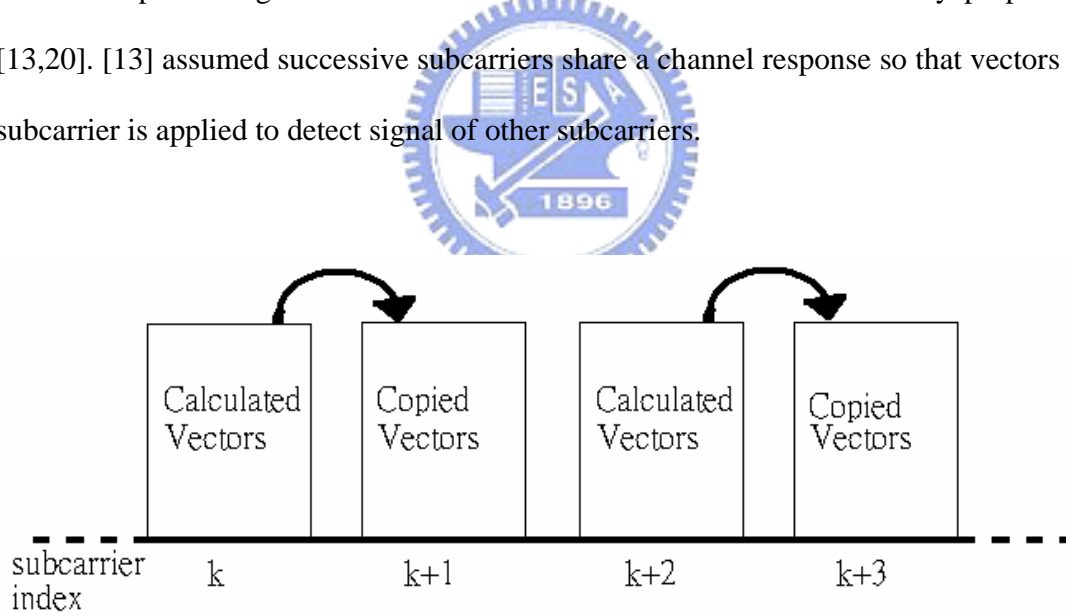


Figure 4.3 The simplified V-BLAST detection algorithm in [13]

In [20], the simplification, however, miss an important assumption. The subcarrier which is decoded by approximation is assumed to have the same decode order with that of the subcarrier which provides the pseudo inverse. At each step of V-BLAST, a column

of channel matrix is set to zero in order to ignore the effect of the corresponding transmitting antenna. If the pseudo inverse is used to estimate inverse of other subcarriers, the subcarriers have to recognize the nulled columns, which stand for detected signals. In other words, the optimal decoding order is assumed not to change.

Under this assumption, there are some opportunities for further simplification. The simplified algorithm has identical performance but with lower complexities. Owing to unchanged decoding order, what we need is merely a row of the approximated pseudo inverse which represents the transmitted signal to be detected, rather than the inverse, as shown below.

$$\left[H(k+1, p)^+ \right]_j \approx \left[H(k, p)^+ + H(k, p)^+ (H(k, p) - H(k+1, p)) H(k, p)^+ \right]_j \quad (4.2)$$

where $[\]_j$ denotes the j -th row.

$$\left[H(k+1, p)^+ \right]_j \approx \left[H(k, p)^+ \right]_j + \left[H(k, p)^+ (H(k, p) - H(k+1, p)) H(k, p)^+ \right]_j \quad (4.3)$$

then

$$\left[H(k+1, p)^+ \right]_j \approx \left[H(k, p)^+ \right]_j + \left[H(k, p)^+ \right]_j (H(k, p) - H(k+1, p)) H(k, p)^+ \quad (4.4)$$

As a result, computation complexity is simplified, but performance is not degraded because the basis approximation remains unchanged.

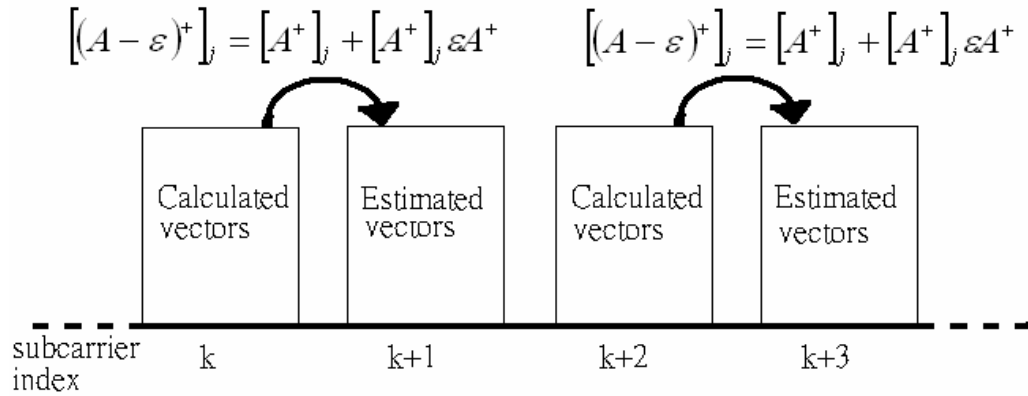


Figure 4.4 Scenario of the proposed simplified V-BLAST detection algorithm

```

Begin
for(i=1 ; i <= subcarrier number ; i+=2)                                (4.5.a)
    calculate weight vectors  $g_{ZF}^i$  according to equation 2.13          (4.5.b)
    if algorithm [13]                                                    (4.5.c)
         $g_{ZF}^{i+1} = g_{ZF}^i$                                           (4.5.d)
    else //algorithm 2                                                  (4.5.e)
        calculate weight vectors  $g_{ZF}^{i+1}$  according to equation 4.4    (4.5.f)
    end                                                                    (4.5.g)
end                                                                        (4.5.k)

```

4.3 The Simplified SQRD Detection Methods

Like V-BLAST algorithm, transmitted signals are detected one by one in SQRD algorithm. Also, optimal detection order of a subcarrier is assumed to be the same with the subcarrier which provides QR decomposition. Our proposed simplified algorithm 1 for SQRD detection is that for each two subcarriers, we compute QR decomposition of one subcarrier using SQRD algorithms [10,11], and applied it to detect the other subcarrier, too.

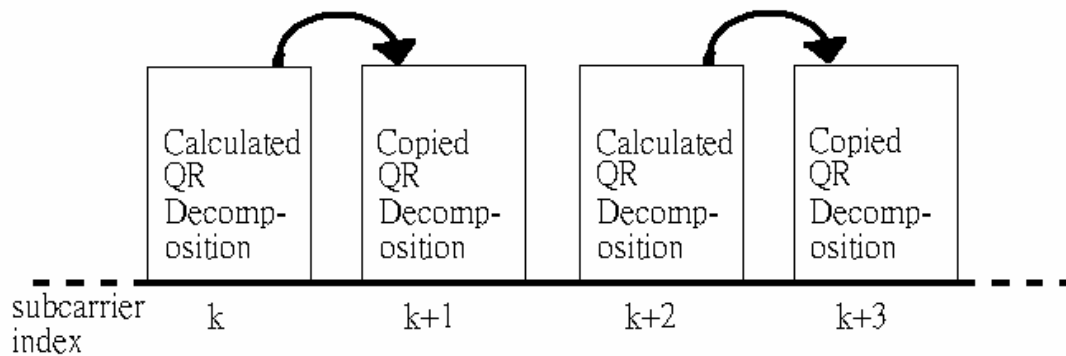


Figure 4.5 Scenario of the proposed simplified SQRD detection algorithm 1

Due to simplicity consideration, we assume the channel response of a subcarrier has the same Q matrix and different R matrix with that of neighboring subcarriers.

Assume that

$$H = QR \quad (4.6)$$

is calculated for one subcarrier. According to previous assumption,

$$H' = QR' \quad (4.7)$$

is the channel response of the neighboring subcarrier. Therefore, R matrix must be updated by R' matrix.

$$y' = H'x' \quad (4.8)$$

where x' and y' mean the transmitted data and the received data of the neighboring subcarrier, respectively. We can simply multiply Q^H matrix with both sides of equation 4.5.

$$Q^H y' = Q^H H' x' \quad (4.9)$$

It is known that each column of Q is orthogonal to each other. That is,

$$Q^H Q = I \quad (4.10)$$

then

$$Q^H H = Q^H QR' = IR' = R' \quad (4.11)$$

Equation 4.9 can be re-written as

$$Q^H y' = R' x' \quad (4.12)$$

Our proposed simplified algorithm 2 for SQRD detection method is that for each two subcarriers, we compute QR decomposition of one subcarrier using SQRD algorithms [10,11], and then we approximate the other by updating R matrix.

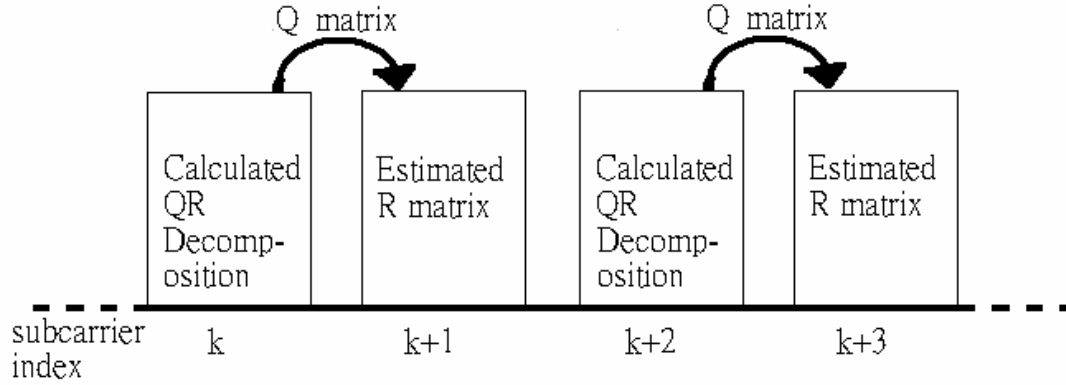


Figure 4.6 Scenario of the proposed simplified SQRD detection algorithm 2

Begin

for($i=1$; $i \leq$ subcarrier number ; $i+=2$) (4.5.a)

calculate Q^i R^i according to [10,11] (4.5.b)

if algorithm 1 (4.5.c)

$Q^{i+1} = Q^i$, $R^{i+1} = R^i$ (4.5.d)

else //algorithm 2 (4.5.e)

$Q^{i+1} = Q^i$, $R^{i+1} = (Q^i)^H H^{i+1}$ (4.5.f)

end (4.5.g)

end (4.5.k)

4.4 Complexity Analysis and Comparison

It is known that the signal detection and calculation of pseudo inverse of a channel are independent. Inverse of a channel only needs to be calculated once when the channel is estimated, and then, as long as the channel does not change, all we need to do is to use the same inverse to detect signal for different data symbols. Accordingly, two parts are separately analyzed.

4.4.1 Number of Complex Multiplications

In these tables, linear denotes direct calculation of pseudo inverse of channel response, APP-Linear denotes the method of using equation 3.1 to estimate pseudo inverse, SQRD denotes direct calculation of QR decomposition according to [10,11], APP-SQRD denotes the method of calculating R' matrix according to equation 4.11, VBLAST denotes calculation of weight vectors using the technique of [8] and APP-VBLAST corresponds to the calculation based on equation 4.4, which results in less complexity than [20]. All ZAPP algorithms denote the no calculation of pseudo inverse, QR decomposition or weight vectors but adopt the closet neighboring ones.

Table 4.1 Multiplication complexities of various detection algorithms for channel inversion

	No. Multiplications	Square Root	Real Division	$N_t=4$ $N_r=6$
Linear	$N_t^3 + 2N_t^2N_r$	0	0	256
APP	$2N_t^2N_r$	0	0	192
ZAPP	0	0	0	0
VBLAST	$N_t^4 + 2N_t^3N_r + N_t^2N_r$	0	0	768
APP	$2N_t^2N_r$	0	0	192
ZAPP	0	0	0	0
SQRD	$N_t^2N_r + 8N_tN_r + 0.5N_t^2 + 1.5N_t$	N_tN_r	$2N_tN_r$	302
APP	$N_t^2N_r$	0	0	96
ZAPP	0	0	0	0

Table 4.1 shows the required numbers of multiplications for channel inversion. In SQRD algorithms, square root and real division is modeled as 7 and 2 complex multiplications, respectively. V-BLAST algorithm needs the most multiplication due to the required N_t pseudo inversion. In comparison, all the ZAPP algorithms need no calculation, because it is just a copy from the quantity of the closet subcarrier.

Table 4.2 Multiplication complexities of various detection algorithms for data detection

	No. Multiplications	$N_t=4$ $N_r=6$	6 symbols
Linear	$N_t N_r$	24	400
APP	$N_t N_r$	24	336
ZAPP	$N_t N_r$	24	144
VBLAST	$N_t^2 + N_t N_r$	40	1008
APP	$N_t^2 + N_t N_r$	40	432
ZAPP	$N_t^2 + N_t N_r$	40	240
SQRD	$N_t N_r + 0.5 N_t^2 + 3.5 N_t$	46	578
APP	$N_t N_r + 0.5 N_t^2 + 3.5 N_t$	46	372
ZAPP	$N_t N_r + 0.5 N_t^2 + 3.5 N_t$	46	276

Table 4.2 shows the required numbers of multiplications for data detection. Since signal detection algorithms are the same for the linear detection algorithm, the three conditions have identical complexity, and so are V-BLAST and SQRD. 6 symbols mean the total required numbers of multiplications for 1-symbol channel inversion and data detection for 6 symbols, assuming that the subcarrier channel response is invariant for the duration of 6 symbols. For $N_t = 4$, $N_r = 6$ and 6 symbols, the parameters are chosen for simulation for apparent difference on complexities and BER performance.

4.4.2 Number of Complex Additions

Table 4.3 Addition complexities of various detection algorithms for channel inversion

	No. additions	$N_t=4$ $N_r=6$
Linear	$N_t^3 + 2 N_t^2 N_r$	256
APP	$2 N_t^2 N_r$	192
ZAPP	0	0
VBLAST	$N_t^4 + 2 N_t^3 N_r + N_t^2 N_r + N_t^2$	784
APP	$3 N_t^2 N_r + N_t N_r$	312
ZAPP	0	0
SQRD	$N_t^2 N_r + 2 N_t N_r + N_t^2 + N_t$	164
APP	$N_t^2 N_r$	96
ZAPP	0	0

Table 4.4 Addition complexities of various detection algorithms for data detection

	No. Multiplications	$N_t=4$ $N_r=6$	6 symbols
Linear	$N_t N_r$	24	400
APP	$N_t N_r$	24	336
ZAPP	$N_t N_r$	24	144
VBLAST	$N_t^2 + N_t N_r$	40	1008
APP	$N_t^2 + N_t N_r$	40	432
ZAPP	$N_t^2 + N_t N_r$	40	240
SQRD	$N_t N_r + 0.5 N_t^2 + 0.5 N_t$	34	368
APP	$N_t N_r + 0.5 N_t^2 + 0.5 N_t$	34	300
ZAPP	$N_t N_r + 0.5 N_t^2 + 0.5 N_t$	34	204

Table 4.3 and Table 4.4 show the required numbers of addition for channel inversion and data detection, respectively. Owing to the fact that a complex multiplication needs much more computation cost than a complex addition, we think the number of multiplication will dominate computation time.



Chapter 5

Simulation Results

In this chapter, we conduct computer simulations and test the performance of the discussed algorithms in Chapter 3 and 4 by using Matlab program. Those simulations are performed by applying them to WWiSE proposal. Table 5.1 lists the parameter settings of WWiSE in the simulations including frame structure, multi-antenna preambles format, signal bandwidth, subcarrier number, et cetera. Modulation scheme is fixed to QPSK and channel coding is neglected. It is also assumed that channel state information (CSI) is perfectly known during the periods of preambles.

First of all, based on the previously mentioned complexity analysis, simulation time is examined. Then an important part, bit error rate (BER), is simulated. Computation time indicates complexity while BER indicates performance.

Table 5.1 Simulated WWiSE system parameters

Signal bandwidth	20MHz
Sample duration	50ns
FFT length	64
Used subcarriers	52
Data subcarriers	48
Symbol period	3.2us (64 samples)
Cyclic prefix	0.8us (16 samples)
Subcarrier spacing	312.5 kHz
Modulation	QPSK
Channel Coding	No
Transmit antenna	4
Receive antenna	4, 5, or 6
Data symbol	6 symbols
Doppler frequency	150 (9m/s at 5GHz)

5.1 Performance – Execution Time

In the following figures, computation time is measured in seconds using Matlab etime functions. Only signal detection is measured and other parts are not, because we are only interested in complexity of detection. 4 transmit and 6 receive antennas are assumed with the theoretically analyzed complexities. In the table, the fractional numbers represent the ratio normalized to the methods of linear, SQRD or V-BLAST, respectively.

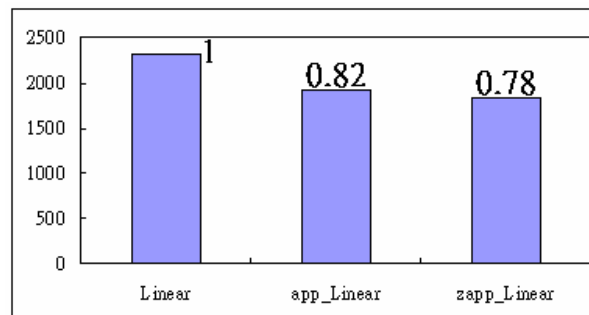


Figure 5.1 Computation time of the linear detection method and its new simplified methods

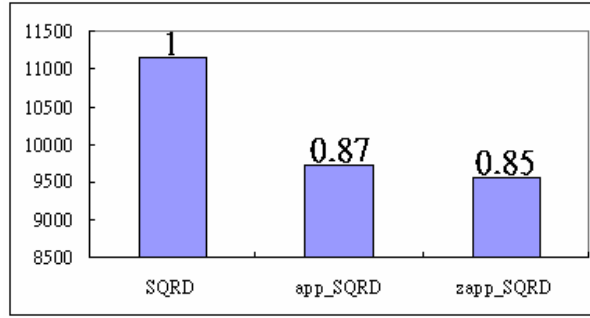


Figure 5.2 Computation time of the SQRD detection method and its new simplified methods

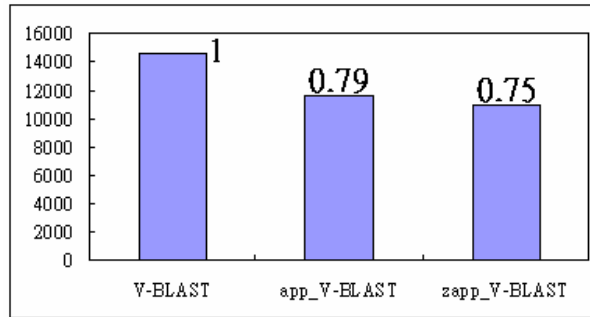


Figure 5.3 Computation time of the V-BLAST detection method and its new simplified methods

It shows that the time saving is not apparent, and contradictory to our previous much simplified complexity analysis. There may be some reasons for this. For all the proposed simplified algorithms, we directly compute channel inverse of the representing subcarrier and use it to approximate the other. Take V-BLAST for example, according to Table 4.2 the normalized complexity of the simplified algorithm with respect to the original one is,

$$\frac{1008 + 432}{2 * 1008} = 0.71 > 0.5 \quad (5.1)$$

We divide the total multiplication numbers of APP-VBLAST by that of the pure V-BLAST detections. As shown, a complexity saving of more than 0.5 is impossible

because for every two subcarriers, the channel inverse of one subcarrier is directly computed so that there is no saving for this subcarrier. Besides the computer simulation result shows further degradation.

$$0.79 > 0.71 \quad (5.2)$$

For computer simulations, a program may consist of lots of memory accesses. Actually, a large memory is essential to run the new algorithms. For example, APP-VBLAST needs pseudo inverse in each operation step for approximation. That is, for the simulated 4 transmit and 6 receive antennas systems, four 6 by 4 pseudo inverse matrixes should be stored in a memory and accessed.

5.2 Performance – Bit Error Rate

In our discussion, correlations between transmit antennas and that between receive antennas are assumed to be independent, and each transmit and receive antenna pair follows the same channel model. In the BER simulations, indoor channel model [23] is adopted because both 802.11n and 802.11a focus similar on indoor wireless applications, and the simulated channel is generated by a hand-written program using Jake's model. As shown before, a simulated packet consists of preamble part and 6 data symbols. In our simulation, perfect channel state information (CSI) is adopted.

The first simulated channel, as listed in Table 5.2, is measured in a typical old office environment where partitions are often made of brick. The longest tap has a delay of 127ns, which is about 2.5 samples for 802.11a system. The delay is so small that a very large coherent bandwidth is expected.

Table 5.2 Indoor channel model [23] with short delays, office

Tap No.	Delay (ns)	Power (dB)	Amplitude Distribution	Doppler Spectrum
1	0	0	Rayleigh	Classical/Flat
2	36	-5	Rayleigh	Classical/Flat
3	84	-13	Rayleigh	Classical/Flat
4	127	-19	Rayleigh	Classical/Flat

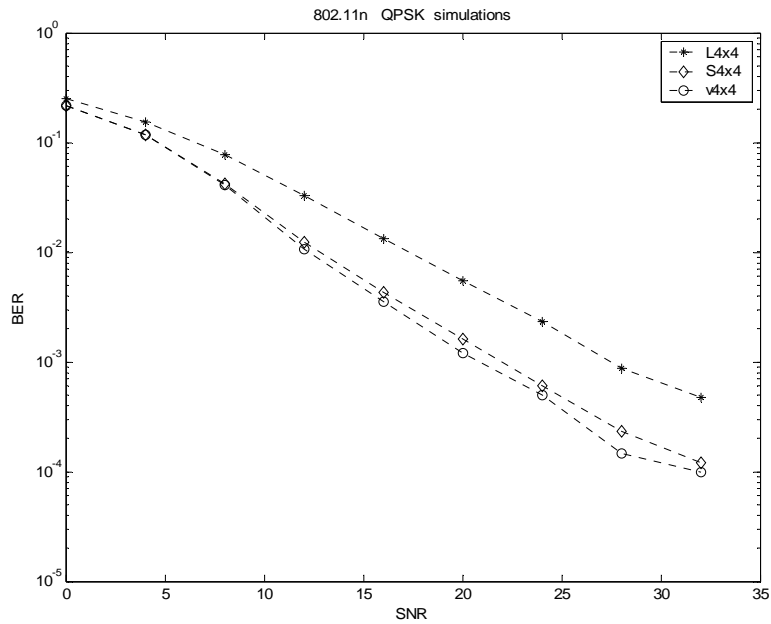


Figure 5.4 BER performance versus detection techniques (4x4), office

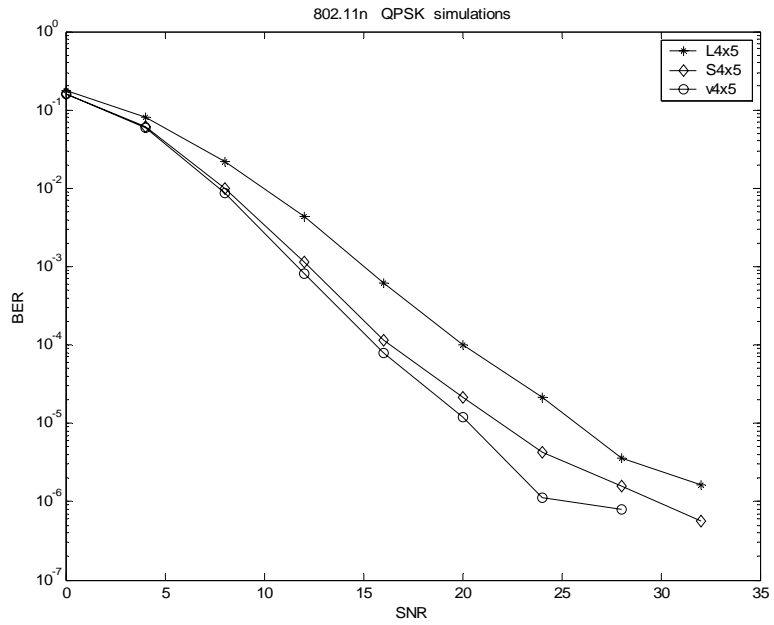


Figure 5.5 BER performance versus detection techniques (4x5), office

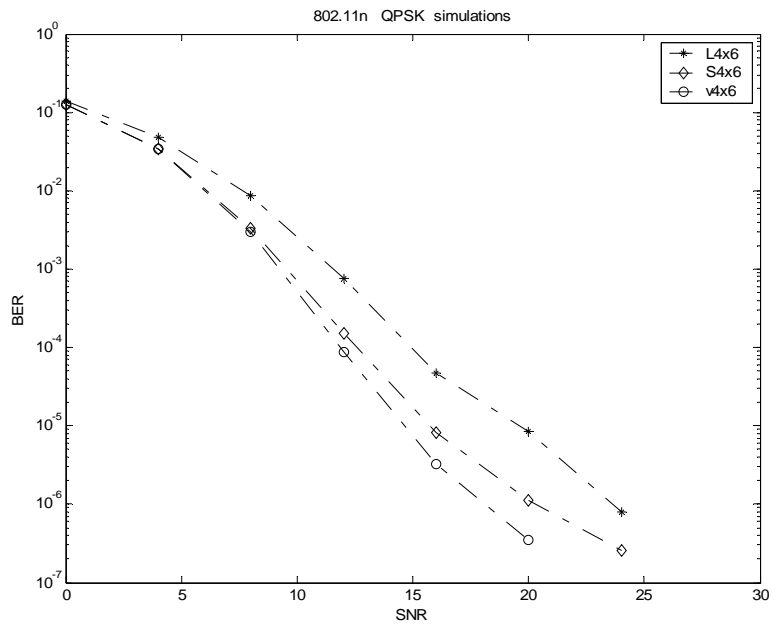


Figure 5.6 BER performance versus detection techniques (4x6), office

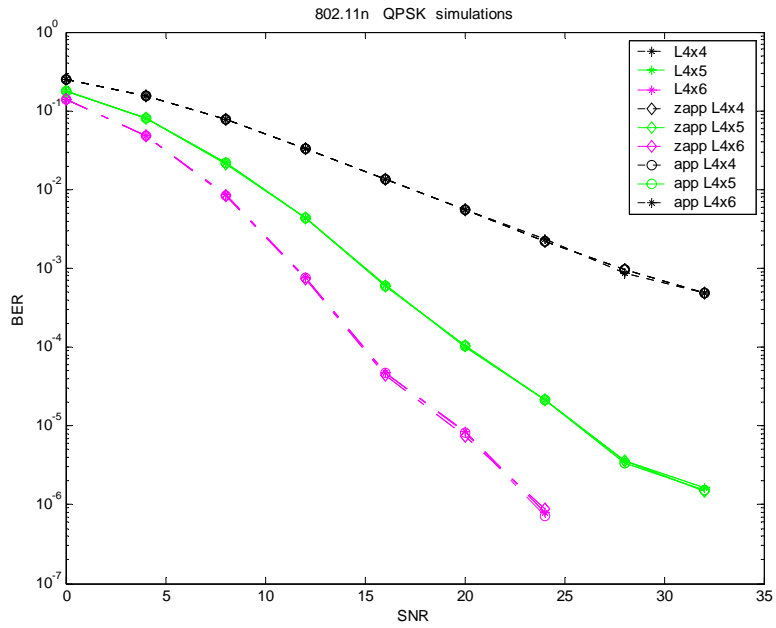


Figure 5.7 BER performance versus the linear detection method and the proposed approximation method, office

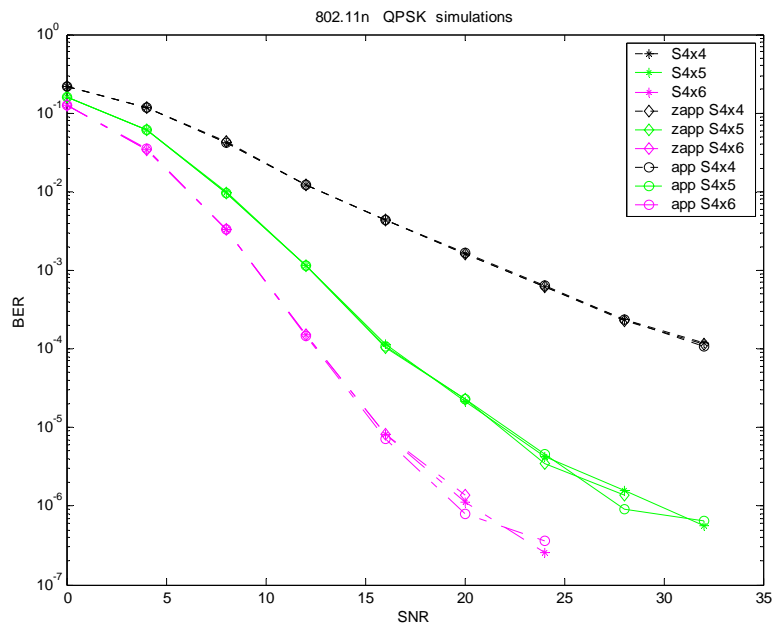


Figure 5.8 BER performance versus the SQRD detection method and the proposed approximation method, office

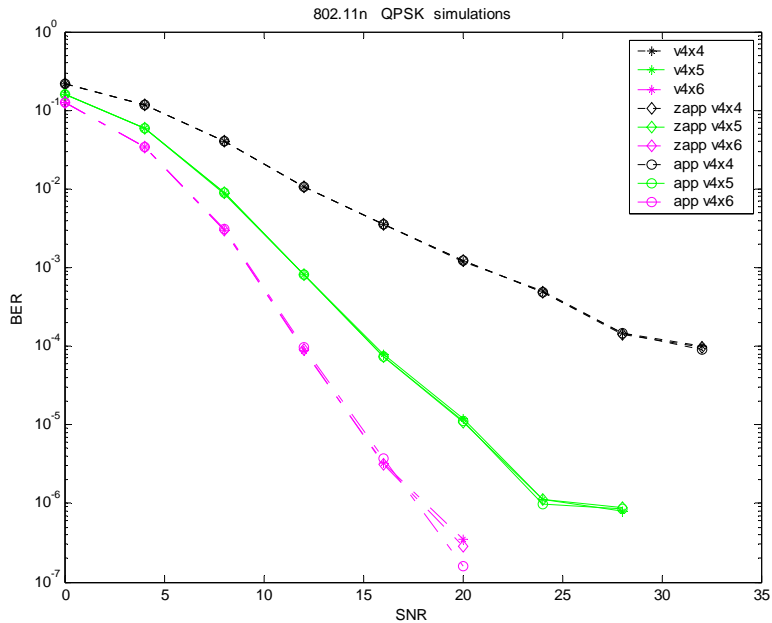


Figure 5.9 BER performance versus the V-BLAST detection method and the proposed approximation method, office

Figure 5.4 shows performances of various techniques. L denotes linear detection, S denotes SQRD detection, and V denotes V-BLAST detection. In Figure 5.5, 4x5 means that there are 4 transmit and 5 receive antennas. Similarly and etc for Figure 5.6 It is obvious that V-BLAST has the best performance and linear has the worst, as mentioned in Section 2.3.

Figure 5.7 shows performances of the linear detection method and the proposed approximation method. Here we use similar notations as Section 5.1. There are similar notations in Figure 5.8 and 5.9.

As shown in the figures, there is no performance difference the between original algorithms and their simplified algorithms. The condition is also observed in Figure 5.8

and Figure 5.9. This is maybe because the channel model has very short delays and thus a very wide coherent bandwidth.

The second simulated channel is measured in an airport representing a typical large hall area. The channel has a few very long delay paths which indicate bad channel conditions and is harmful to communication.

Table 5.3 Indoor channel model [23], large hall

Tap No.	Delay (ns)	Power (dB)	Amplitude Distribution	Doppler Spectrum
1	0	0	Rayleigh	Classical
2	174	-8	Rayleigh	Classical
3	274	-15	Rayleigh	Classical
4	560	-18	Rayleigh	Classical

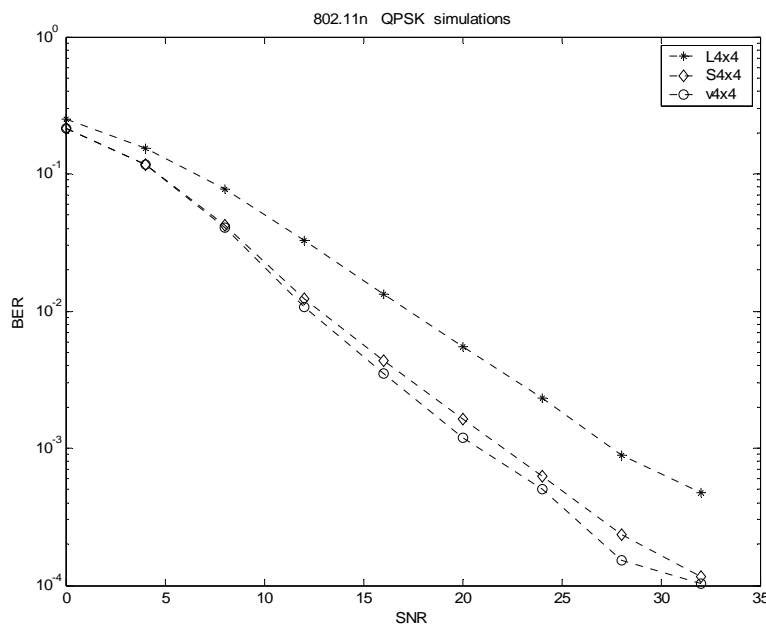


Figure 5.10 BER performance versus detection techniques (4x4), large hall

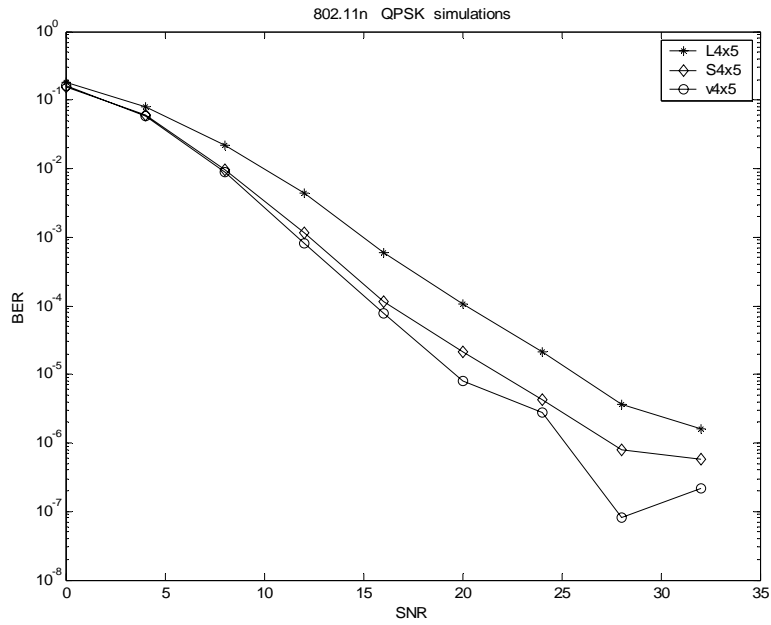


Figure 5.11 BER performance versus detection techniques (4x5), large hall

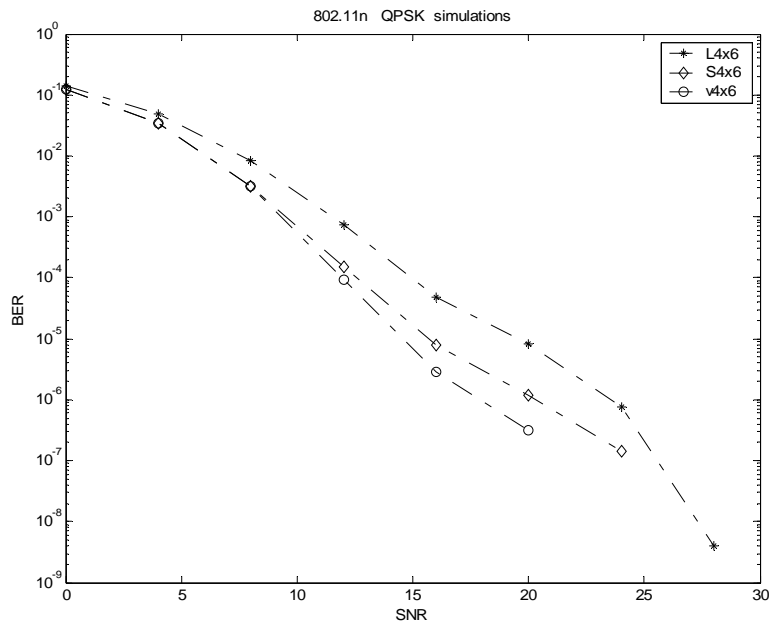


Figure 5.12 BER performance versus detection techniques (4x6), large hall

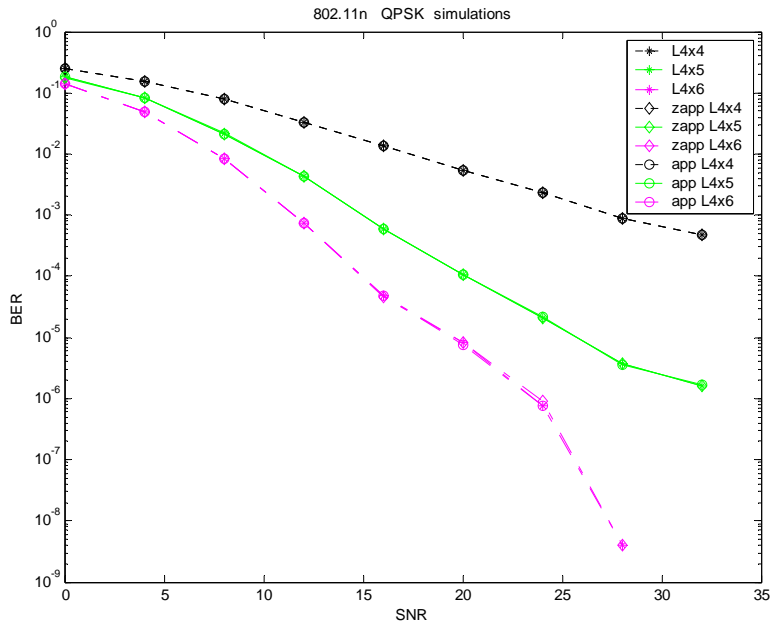


Figure 5.13 BER performance versus the linear detection method and the proposed approximation method, large hall

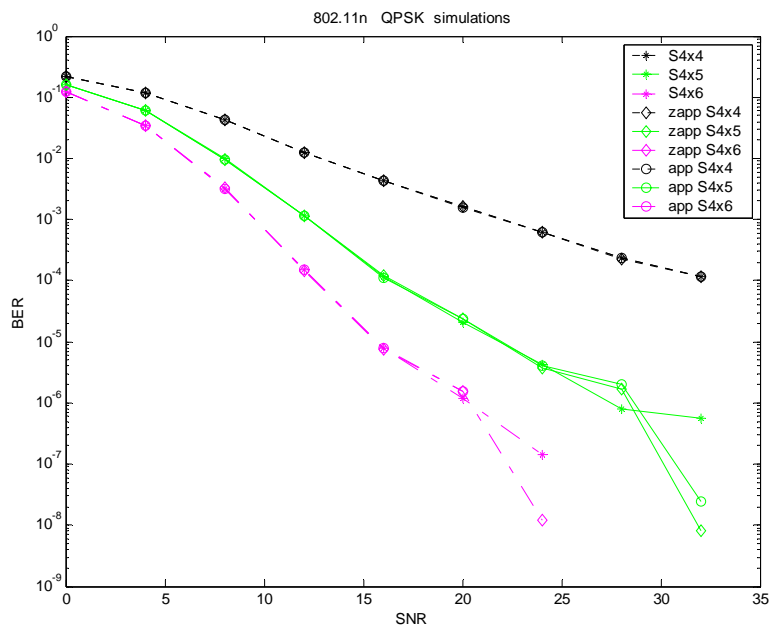


Figure 5.14 BER performance versus the SQRD detection method and the proposed approximation method, large hall

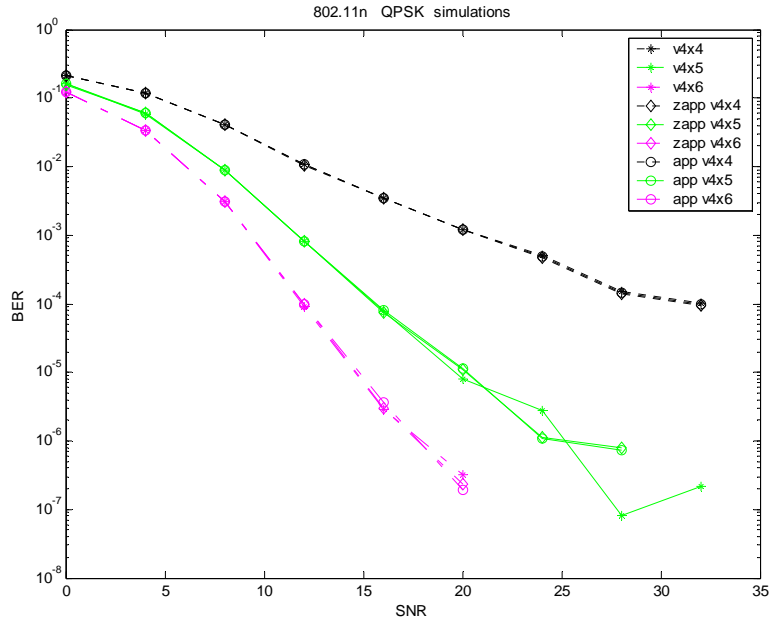


Figure 5.15 BER performance versus the V-BLAST detection method and the proposed approximation method, large hall

Figure 5.10 shows performances of various techniques under channel model of large hall. It shows the similar performance trends as in Figure 5.4. Surprisingly, Figure 5.13, Figure 5.14 and Figure 5.15 show no difference between original algorithm and the simplified algorithms. The reason may be as follows.

It is known that within coherent bandwidth, channel frequency response can be viewed as flat. Coherent bandwidth is inversely proportional to channel delay spread [24].

$$B_c \approx \frac{1}{\tau_{rms}} \quad (5.1)$$

In OFDM systems, the maximum endurable channel delays are the length of cyclic prefix, which represents the worst channel condition. Of course, the maximum delay of a channel is larger than its delay spread.

$$\tau_{max} > \tau_{rms} \quad (5.2)$$

Then

$$Bc \approx \frac{1}{\tau_{rms}} > \frac{1}{\tau_{max}} \quad (5.3)$$

Let OFDM signal bandwidth be M , FFT length be N , cyclic prefix length be $\frac{N}{K}$, and the subcarrier spacing be $\frac{M}{N}$. Assume the maximum channel delay equals to the cyclic prefix length, which stands for the worst channel condition.

$$\tau_{max} = \frac{N}{K} \times \frac{1}{M} \quad (5.4)$$

where $\frac{1}{M}$ represents sampling period.

Then

$$Bc \approx \frac{1}{\tau_{rms}} > \frac{1}{\tau_{max}} = \frac{KM}{N} \quad (5.5)$$

By dividing both side by subcarrier spacing $\frac{M}{N}$, we have

$$Bc \frac{N}{M} > K \quad (5.6)$$

Coherent bandwidth divided by subcarrier spacing defines the number of subcarriers which has the same channel response. According to equation 5.6, the number is larger than K , so K consecutive subcarriers can be seen to have the same channel response. For example, 802.11n system has FFT length 64 and cyclic prefix length 16. Hence, 4 consecutive subcarriers can be seen to have the same channel response. As a result, undoubtedly the proposed simplified algorithms result in no performance degradation compared to the original algorithms. Furthermore, the proposed algorithms can potentially save more computation complexities by considering every 4 consecutive

subcarriers as a group shares the same channel response. And this better consideration is remained to be verified.

To understand influence of non-perfect channel knowledge, simulations with added channel noise are finished. This adopts the V-BLAST algorithm and the same parameters as the large hall.

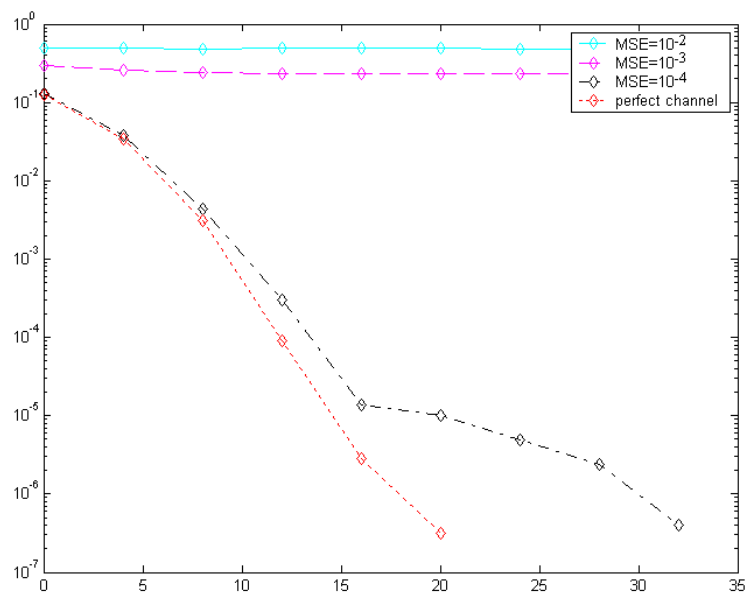


Figure 5.16 BER performance versus channel MSE, large hall

The figure shows that the non-perfect channel estimation will degrade the performance very apparently. If channel estimation is not well designed, V-BLAST algorithm may not be useful in MIMO OFDM systems.

Chapter 6

Conclusion

In this thesis, new simplified algorithms for various well known MIMO OFDM detection techniques are proposed, followed by a thorough investigation and verifications in terms of complexity and BER performance by testing WWiSE systems. Although V-BLAST algorithm results in the best performance, it demands the highest computation cost. Since designs of detection methods are trade-off problems between cost and performance, complexity and performance analysis helps a lot to decide a suitable design.

Some extended property about coherence bandwidth is proposed, which predicts the minimum number of consecutive subcarriers which share the same channel response. Since when a channel response is shared, channel inversion can be computed for those related subcarriers. It helps to reduce system complexity without loss of BER performance and makes V-BLAST implementation on OFDM systems possible.

It is well known that MMSE criterion results in better performance than ZF criterion and thus is considered as future work. Detection algorithms about MMSE criterion are going to be investigated and extended for lower complexity and better

performance. Besides, data detection is performed in frequency domain because the FFT output can be modeled as linear transformation of IFFT input. It is also future work to search for a method that can perform data detection in time domain. Under slow fading channels, the FFT output is linear transformation of IFFT input, but under fast fading channels, this is not the case. It is originally a challenging task to model the time varying channel. If taking both fast fading channel modeling and signal detection into consideration, the problem is even bigger and is interesting for research. It is also referred to as future work to find out some algorithms reach low complexity and solve this challenging problem.



Bibliography

- [1] T. Ojanpera and R. Prasad, "An overview of wireless broadband communications," IEEE Commun. Mag. Vol.35, No. 1, pp. 28-34, Jan 1997.
- [2] C. L.Ng, K. B. Letaief, and R.D. Murch, "Antenna diversity combining and finite-tap decision feedback equalization for high-speed data transmission," IEEE Journal on Selected Areas in Communication, Vol. 16, No.8, pp. 1367-1375, Qct. 1998.
- [3] B. Yang, K .B. Latief, R. S. Cheng, and Z. Cao, "Channel estimation for OFDM transmission in multipath fading channels based on parameter channel modeling," IEEE Transations on Communications, Vol. 49, No. 3, March 2001.
- [4] W. K. Wang, R. S. Cheng, K. B. Latief, and R. D. Murch, "Adaptive antennas at the mobile and base station in an OFDM/TDMA systems," IEEE Transactions on Communications, Vol. 49, No.1, Jan. 2001.
- [5] C. Y. Yue, R. S. Cheng, K. B. Letaief, and R. D. Murch, "Multiuser OFDM with subcarrier, bit, and power allocation," IEEE Journal On Selected Areas in Communications, Vol. 17, No. 10, pp. 1747-1758, October 1999.
- [6] G. J. Foschini and M. J. Cans, "On limits of wireless communications in a fading environment when using multiple antennas," Wireless Personal Communications, Vol. 6, NO. 3, pp. 311-335, 1998.
- [7] G. G. Raleigh and J. M. Cioffi, "Spatio-temporal coding for wireless communication," IEEE Trans. Communications, Vol. 46, No. 3, pp. 357-366, March 1998.

- [8] G. J. Foschini, "Layered space-time architecture for wireless communication in a fading environment when using multiple antennas," Bell laboratories Technical Journal, Vol. 1, No. 2, pp. 41-59, 1996.
- [9] P. W. Wolniansky, G. J. Foschini, G. D. Golden, R. A. Valenzuela, "V-BLAST an architecture for realizing very high data rates over the rich-scattering wireless channel," Invited paper; Proc. ISSSE-98, Pisa, Italy, 1998.
- [10] D. Wubben, R. Bohnke, J. Rinas, V. Kuhn, and K. D. Kammeyer, "Efficient algorithm for decoding layered space-time codes," Electronics Letters, Volume 37, Issue 22, 25 Oct 2001 Page(s): 1348 - 1350
- [11] D. Wubben, R. Bohnke, V. Kuhn, and K. D. Kammeyer, "MMSE extension of V-BLAST based on sorted QR decomposition," Vehicular Technology Conference, 2003, VTC 2003-Fall, 2003 IEEE 58th Volume 1, 6-9 Oct. 2003 Page(s): 508 - 512 Vol.1.
- [12] N. Boubaker, K. B. Letaief, and R. D. Murch, "A layered space-time coded wideband OFDM architecture for dispersive wireless links," Computers and Communications, 2001, Proceedings, Page(s): 518 – 523, July 2001
- [13] N. Boubaker, K. B. Letaief, R. D. Murch, "A low complexity multicarrier BLAST architecture for realizing high data rates over dispersive fading channels," VTC 2001 Spring, IEEE VTS 53rd Volume 2, Page(s): 800 - 804 vol.2, 6-9 May 2001.
- [14] Ye Li, J.C. Chuang and N.R. Sollenberger, "Transmitter diversity for OFDM systems and its impact high rate data wireless networks," IEEE Journal on Selected Areas in Communications, Vol. 17, NO. 7, pp. 1233-1243, July 1999.

- [15] S.B. Bulumulla, S.A. Kassam and S.S. Venkatesh, "An adaptive diversity receiver for OFDM in fading channels," IEEE Int. Conf. on Communications 88, Proc. 1998, Vol. 3, pp. 1325-1329.
- [16] Gong Yi and K. B. Letaief, "Performance evaluation and analysis of space-time coding in unequalized multipath fading links," IEEE Transactions on Communications, Vol. 48, pp. 1778-1782, Nov. 2000.
- [17] Jiann-Jong Wang and Ta-Sung Lee "Applications of dynamic subcarrier allocation and adaptive modulation in multiuser MIMO-OFDM systems" Institute of Communication Engineering, Hsinchu, Taiwan, National Chiao Tung University, 2004.
- [18] S. Verdu, Multiuser Detection, 2nd ed. Cambridge, U.K.: Cambridge University Press, 1998.
- [19] J. Silverstein and Z. Bai, "On the empirical distribution of eigenvalues of a class of large dimensional random matrices," Journal of Multivariate Analysis, vol. 54, no. 2, pp. 175-192, 1995.
- [20] Qianlei Liu, and Luxi Yang, "A simplified method for V-BLAST detection in MIMO OFDM communication" Communications, 2004 and the 5th International Symposium on Multi-Dimensional Mobile Communications Proceedings. The 2004 Joint Conference of the 10th Asia-Pacific Conference on Volume 1, 29 Aug.-1 Sept. 2004 Page(s): 30 - 33 vol.1.
- [21] <http://www.WWiSE.org/>
- [22] IEEE Std 802.11a-1999, Wireless LAN Medium Access Control (MAC) and Physical Layer (PHY) Specifications, 1999 edition.

- [23] X. Zhao, J. Kivinen, and P. Vainnikainen, "Tapped delay line channel models at 5.3 GHz in indoor environments," Vehicular Technology Conference, 2000. IEEE VTS-Fall VTC 2000. 52nd Volume 1, 24-28 Sept. 2000 Page(s): 1 - 5 vol.1.
- [24] A. Paulrajm, R. Nabar, and D. Gore, Introduction to Space-Time Wireless Communications, 1st ed. Cambridge, U.K.: Cambridge University Press, 2003.

